



**Ultra-frequent HRAS p.Q61R somatic mutation in canine acanthomatous ameloblastoma reveals pathogenic similarities with human ameloblastoma**

Journal:	<i>Veterinary and Comparative Oncology</i>
Manuscript ID	Draft
Manuscript Type:	Short Communication
Keywords:	ameloblastoma, animal model, canine acanthomatous ameloblastoma, HRAS, oncogenic mutation, odontogenic tumor

SCHOLARONE™  
Manuscripts



## Ultra-frequent *HRAS* p.Q61R somatic mutation in canine acanthomatous ameloblastoma reveals pathogenic similarities with human ameloblastoma

### Abstract

Ameloblastoma is a locally aggressive odontogenic tumor that occurs in humans and dogs. Most ameloblastomas in humans (AM) harbor mutually-exclusive driving mutations in *BRAF*, *HRAS*, *KRAS*, *NRAS* or *FGFR2* that activate MAPK signaling. The remarkable clinical and histological similarities between canine acanthomatous ameloblastoma (CAA) and AM suggest they may harbor similar driving mutations, yet no studies have investigated these genes in CAA. Here we demonstrate that 94% of CAA harbor a somatic *HRAS* p.Q61R mutation, suggesting that the molecular mechanisms of tumorigenesis are conserved, and thus qualifying the dog as a potentially useful model of disease. Given the relevance of *RAS* mutations in the pathogenesis of odontogenic tumors and other types of cancer, the results of this study are of comparative, translational, and veterinary value.

Keywords: ameloblastoma; animal model; canine acanthomatous ameloblastoma; *HRAS*; oncogenic mutation; odontogenic tumor.

1  
2  
3 Ameloblastoma is an odontogenic tumor that occurs in humans and dogs.<sup>1-3</sup> As in  
4  
5 humans, ameloblastomas in dogs are more common in the mandible than in the maxilla,  
6  
7 and are typically locally aggressive and destructive (**Figure 1**).<sup>3</sup> The standard of care for  
8  
9 ameloblastomas has traditionally been wide surgical excision of the affected area of the  
10  
11 mandible or maxilla.<sup>4,5</sup> However, surgery is highly invasive and may result in significant  
12  
13 disfigurement and dysfunction.<sup>6,7</sup> Novel therapeutic approaches based on molecular  
14  
15 oncogenic mechanisms are expected to replace or complement current surgical  
16  
17 solutions and thus help minimize patient morbidity while improving possible outcomes.<sup>8</sup>  
18  
19  
20  
21  
22  
23

24 Human ameloblastomas (AM) express early dental epithelial transcription factors such  
25  
26 as *PITX2*, pointing out to the origin from a dental laminal cell.<sup>9</sup> Recent discoveries have  
27  
28 shown that the majority of AM are driven by mutually-exclusive *BRAF*, *HRAS*, *NRAS*,  
29  
30 *KRAS* or *FGFR2* mutations that activate the MAPK pathway regulating cell survival.<sup>7,10-</sup>  
31  
32  
33 <sup>14</sup> Co-occurring *SMO* mutations that alter the Hedgehog signaling pathway to regulate  
34  
35 cell fate have also been detected, especially in maxillary tumors.<sup>11,12</sup> Both pathways are  
36  
37 mutated in various cancers and have been targeted for therapy, making them of  
38  
39 particular interest in modern oncology.<sup>7</sup>  
40  
41  
42  
43  
44

45 Tooth development is similar in humans and dogs, and AM and canine acanthomatous  
46  
47 ameloblastomas (CAA) show remarkable clinical and histological and similarities.<sup>3,13,15</sup>  
48  
49 Therefore, it is likely that both tumors harbor similar oncogenic mutations. The purpose  
50  
51  
52  
53  
54  
55  
56  
57  
58  
59  
60

1  
2  
3  
4 of this study was to determine whether CAAs harbor any of the oncogenic mutations  
5  
6  
7 frequently found in AM.  
8  
9

10 Our study consisted of the molecular characterization of candidate oncogenic mutations  
11  
12 in 16 CAA cases from client-owned dogs (**Table 1**). Eight gingival oral squamous cell  
13  
14 carcinoma (OSCC) tumor samples, as well as 4 healthy gingival samples, all from  
15  
16 different dogs, were used as controls. Dog owners signed an informed consent for use  
17  
18 of tissues and blood for research purposes prior to collection. Sample collection and  
19  
20 experimental procedures were in accordance with a protocol (#2005-0151) approved by  
21  
22 Cornell University's Institutional Animal Care and Use Committee. All tumors were  
23  
24 confirmed by histological assessment of routine H&E stained formalin-fixed and  
25  
26 paraffin-embedded tumor sample by a board-certified veterinary pathologist (GED)  
27  
28  
29  
30  
31 (**Figure 2**).  
32  
33  
34

35 Frozen study and control tissues were homogenized in Trizol (Thermo Fisher) using a  
36  
37 bead mill without being allowed to thaw. RNA was isolated following the manufacturer's  
38  
39 protocol with the following modifications: an extra chloroform extraction was added prior  
40  
41 to precipitation, 1 µl glycoblue (Thermo Fisher) was added immediately prior to  
42  
43 precipitation, and the RNA pellet was washed twice with 75% ethanol. RNA  
44  
45 concentration was measured with a Nanodrop and integrity determined with a Fragment  
46  
47 Analyzer (AATI).  
48  
49  
50  
51  
52  
53  
54  
55  
56  
57  
58  
59  
60

1  
2  
3 RNAseq libraries were generated with the NEBNext Ultra II Directional library prep kit  
4  
5 (NEB) using 250ng input total RNA. Single-end 85nt reads were generated on a  
6  
7 NextSeq500 instrument (Illumina). Reads were trimmed with cutadapt<sup>16</sup> and mapped to  
8  
9 the CanFam3 reference genome with Tophat<sup>17</sup> v2.1.1 to investigate polymorphisms in  
10  
11 candidate oncogenic driver genes.  
12  
13

14  
15  
16  
17 For Sanger sequencing and restriction fragment length polymorphisms (RFLP)  
18  
19 validation assays, each RNA sample was used to generate cDNA using MMLV reverse  
20  
21 transcriptase (Sigma) according to the manufacturer's instructions in a final 20µl  
22  
23 reaction containing 500ng total RNA, 33uM random nonamer primers, and 25uM oligo-  
24  
25 dT20 primers. The reaction was incubated at 37°C for 1 hour followed by 85°C for 10  
26  
27 minutes to inactivate the reverse transcriptase. Genomic DNA was isolated from EDTA  
28  
29 blood samples by the Cornell Veterinary Biobank using a standard salt precipitation  
30  
31 technique, as previously reported.<sup>18</sup>  
32  
33  
34  
35  
36  
37

38 PCR primers were designed within *HRAS* exon 2 flanking the p.Q61R mutation using  
39  
40 Primer-BLAST11 at NCBI: forward primer ATCGGAAGCAAGTGGTCATCG, reverse  
41  
42 primer ACTGGTGGATGTCCTCAAAGG. Each PCR reaction contained 1x Q5 Hot Start  
43  
44 High Fidelity Master (New England Biolabs), 25uM each PCR primer (IDT), and 1µl  
45  
46 cDNA (from tumor RNA) or 500ng genomic DNA (from blood) in a 50µl reaction volume.  
47  
48 PCR reactions were cycled as follows: denaturation at 98°C/3min; 35 cycles of  
49  
50 98°C/10sec - 62°C/10sec - 72°C/15sec; final extension 72°C/5min. Reactions were  
51  
52 cleaned up with a PCR purification kit (Qiagen buffers, Omega HiBind columns), eluted  
53  
54  
55  
56  
57  
58  
59  
60

1  
2  
3 in 50µl EB, and quantified with a Nanodrop. PCR amplicons were sequenced at the  
4  
5 Cornell BRC Genomics Facility using 8 µl PCR product (120-400ng) combined with  
6  
7 25pmol reverse primer to generate antisense reads across the variant position. KB  
8  
9 Basecaller software was used to compensate for mobility differences between dyes.  
10  
11 Restriction digest reactions containing 45ng PCR product, 1x buffer, 1µl restriction  
12  
13 enzyme (New England Biolabs) in total 20µl reaction volume and were incubated at the  
14  
15 recommended temperature for 20 minutes. Digested samples were run on a native 6%  
16  
17 PAGE gel at 100V for 2 hours and stained with GelStar (Lonza).  
18  
19  
20  
21  
22  
23

24 Analysis of RNA sequencing data identified reads that indicated a possible *HRAS*  
25  
26 missense mutation (A → G) that would alter the protein sequence from glutamine (cAg)  
27  
28 to arginine (cGg) at position 61 (p.Q61R mutation) in 11 of 12 CAA samples, while no  
29  
30 deleterious sequence variants were observed in *BRAF*, *NRAS*, *KRAS*, *FGFR2* or *SMO*  
31  
32 (see **Supporting Information**). To validate the occurrence of the *HRAS* p.Q61R  
33  
34 mutation in CAA, we designed a PCR assay for canine *HRAS* exon 2 flanking the  
35  
36 variant site (amplicon size 168bp) that can be used on either RNA (cDNA) or genomic  
37  
38 DNA samples. The presence of the variant allele was assessed by two different  
39  
40 approaches: Sanger sequencing and RFLP. The presence of the variant allele was  
41  
42 detected by Sanger sequencing in cDNA from 15 of 16 (94%) CAA samples (inclusive  
43  
44 of the 12 samples used for RNA sequencing plus 4 additional independent samples), as  
45  
46 evidenced by a T nucleotide (antisense strand) as well as the wild-type C nucleotide  
47  
48 (**Figure 3; Supporting Information**). To determine whether the mutant allele was  
49  
50 present in other (non-tumor) tissues in some of the same dog or arose within the tumor,  
51  
52  
53  
54  
55  
56  
57  
58  
59  
60

1  
2  
3 we also sequenced genomic DNA isolated from paired blood samples from 7 dogs. All 7  
4  
5 had only the wild-type allele, indicating a somatic mutation occurred in the tumor in each  
6  
7  
8 case.

9  
10  
11  
12 We further investigated these results using RFLP analysis on all 16 CAA samples  
13  
14 available for analysis. We developed RFLP assays for both the mutant and wild-type  
15  
16 alleles: HpaII cuts only the mutant allele (CCGG) to generate bands of 122bp and  
17  
18 46bp; d BstNI cuts the wild-type allele as well as an adjacent invariant site, so the wild-  
19  
20 type allele yields 46bp and 107bp bands, whereas samples harboring the mutant allele  
21  
22 type allele yields 46bp and 107bp bands, whereas samples harboring the mutant allele  
23  
24 have a band at 122bp (the 15bp fragment cut from the wild-type product is not visible on  
25  
26 the gel). In all cases, the RFLP assays were internally consistent and agreed with the  
27  
28 Sanger sequencing, confirming that all but one CAA sample had the mutant allele.  
29  
30 RFLP analysis for the mutant allele (HpaII assay) in genomic DNA from 7 paired blood  
31  
32 samples again confirmed the *HRAS* p.Q61R mutation is somatic and not inherited.  
33  
34  
35  
36  
37

38 To confirm that the *HRAS* p.Q61R mutation was specific to CAA, we performed Sanger  
39  
40 sequencing on 8 gingival OSCC and 4 healthy gingival samples from 12 different dogs.  
41  
42 Oral squamous cell carcinoma was chosen as a control tissue because this tumor type  
43  
44 represents the most common oral malignancy of epithelial origin in dogs, and shares  
45  
46 some histological features with CAA.<sup>6,19,20</sup> Sanger sequencing showed that only wild-  
47  
48 type *HRAS* alleles were present in healthy gingival samples (see **Supporting**  
49  
50 **Information**). All OSCC samples had wild-type *HRAS* alleles except case 22 which  
51  
52  
53  
54  
55  
56  
57  
58  
59  
60



1  
2  
3 showed an *HRAS* p.Q61L mutation, consistent with a previous report showing low  
4  
5 frequency of this mutation in this tumor type.<sup>21</sup>  
6  
7

8  
9  
10 The presence of a somatic *HRAS* p.Q61R mutation in 94% of the CAA tumor samples  
11  
12 analyzed in this study demonstrates that the mutational basis of CAA and AM is  
13  
14 comparable (**Figure 4**), and strongly implicates conserved oncogenic molecular  
15  
16 mechanisms. The known clinical and histological similarities between CAA and AM,<sup>15</sup>  
17  
18 and now the observation of common oncogenic mutations in both species, invokes the  
19  
20 opportunity to leverage dogs as a natural model of this disease. Moreover, given that  
21  
22 *RAS* mutations are also well known drivers of several types of cancer in people,<sup>22</sup> our  
23  
24 findings suggest that dogs may potentially be used as translational models for targeted  
25  
26 treatments of MAPK pathway mutated neoplasms. This is a significant finding  
27  
28 considering that dog models offer many advantages over small and (other) large animal  
29  
30 models (i.e. primates), and can be particularly valuable for drug discovery and  
31  
32 development purposes.<sup>23</sup>  
33  
34  
35  
36  
37  
38  
39

40 The apparent prominent role of *RAS* mutations in tumorigenesis of odontogenic  
41  
42 neoplasms is not unprecedented.<sup>14</sup> Indeed, *RAS* mutant mice have been shown to  
43  
44 develop odontogenic neoplasms.<sup>24</sup> Additionally, most adenomatoid odontogenic tumors  
45  
46 harbor *RAS* mutations.<sup>25</sup> Nevertheless, some interesting comparisons should be made  
47  
48 between CAA and AM, which emphasize the need for additional studies. One notable  
49  
50 difference lies in the frequency of the *HRAS* p.Q61R mutation. Contrasting with our  
51  
52  
53  
54  
55  
56  
57  
58  
59  
60

1  
2  
3 findings, only 20% of AM harbor *RAS* mutations, with *HRAS* p.Q61R occurring with a  
4  
5 frequency of 6% or less.<sup>10-13</sup>  
6  
7

8  
9  
10 Similarly, while two thirds or more of AM harbor a *BRAF* V600E mutation,<sup>10-13</sup>  
11  
12 synonymous mutations have not been identified in CAA,<sup>26</sup> underscoring potentially  
13  
14 significant differences in the mutational profiles. Nevertheless, given that both *BRAF*  
15  
16 and *RAS* mutations activate MAPK signaling,<sup>14</sup> this difference does not necessarily  
17  
18 translate in differences in the biologic mechanisms involved. As well, our findings  
19  
20 suggest that MAPK signaling is involved in both maxillary and mandibular CAA. This  
21  
22 would be consistent with the hypothesis that MAPK activating mutations dominate  
23  
24 oncogenesis of maxillary and mandibular AM, and that *SMO* and other simultaneous  
25  
26 mutations act as secondary drivers.<sup>12</sup>  
27  
28  
29  
30

31  
32  
33 It should be noted that the scope of this pilot study focused on candidate genes known  
34  
35 to be mutated in AM,<sup>10-13</sup> and that it is possible that other genes could be mutated in  
36  
37 CAA tumors, including non-coding RNAs.<sup>27</sup> Furthermore, whether the *HRAS* p.Q61R  
38  
39 allele found in the tumors analyzed in this study acts as a primary or secondary  
40  
41 oncogenic driver cannot be ascertained. Genome-scale mutational analysis as well as  
42  
43 molecular phenotyping will help elucidate ways in which the dog may be a suitable  
44  
45 natural model of AM, or may uncover subtypes of this disease.  
46  
47  
48  
49

50  
51 The veterinary clinical and diagnostic significance of the current study should not be  
52  
53 overlooked in light of its comparative and translational potential. Assays specific to the  
54  
55  
56  
57  
58  
59  
60

1  
2  
3 *HRAS* p.Q61R allele, such as those described here, may offer veterinary diagnostic  
4 potential to distinguish CAA from other oral tumors with overlapping histological features  
5 but different biologic behavior, including OSCC.<sup>6,19,20</sup> Our confirmation of high frequency  
6 MAPK-activating alleles in CAA justifies the investigation of precision-based therapies  
7 for companion dogs that have the potential to mediate disease progression as an  
8 alternative to current invasive and costly surgical treatments.  
9  
10  
11  
12  
13  
14  
15  
16  
17

## 18 **References**

- 19  
20 1. Ebenezer V, Ramalingam B. A cross-sectional survey of prevalence of  
21 odontogenic tumours. *J Maxillofac Oral Surg.* 2010;9(4):369-374.  
22
- 23 2. Walsh KM, Denholm LJ, Cooper BJ. Epithelial odontogenic tumours in domestic  
24 animals. *J Comp Pathol.* 1987;97(5):503-521.  
25
- 26 3. Fiani N, Verstraete FJ, Kass PH, Cox DP. Clinicopathologic characterization of  
27 odontogenic tumors and focal fibrous hyperplasia in dogs: 152 cases (1995-  
28 2005). *J Am Vet Med Assoc.* 2011;238(4):495-500.  
29
- 30 4. White RA, Gorman NT. Wide local excision of acanthomatous epulides in the  
31 dog. *Vet Surg.* 1989;18(1):12-14.  
32
- 33 5. Carlson ER, Marx RE. The ameloblastoma: primary, curative surgical  
34 management. *J Oral Maxillofac Surg.* 2006;64(3):484-494.  
35
- 36 6. Goldschmidt SL, Bell CM, Hetzel S, Soukup J. Clinical characterization of canine  
37 acanthomatous ameloblastoma (CAA) in 263 dogs and the influence of  
38 postsurgical histopathological margin on local recurrence. *J Vet Dent.*  
39  
40  
41  
42  
43  
44  
45  
46  
47  
48  
49  
50  
51  
52  
53  
54  
55  
56  
57  
58  
59  
60

- 1  
2  
3 7. Heikinheimo K, Kurppa KJ, Elenius K. Novel targets for the treatment of  
4 ameloblastoma. *J Dent Res.* 2015;94(2):237-240.  
5  
6
- 7  
8 8. Sauk JJ, Nikitakis NG, Scheper MA. Are we on the brink of nonsurgical treatment  
9 for ameloblastoma? *Oral Surg Oral Med Oral Pathol Oral Radiol Endod.*  
10 2010;110(1):68-78.  
11  
12
- 13  
14 9. Heikinheimo K, Kurppa KJ, Laiho A, et al. Early dental epithelial transcription  
15 factors distinguish ameloblastoma from keratocystic odontogenic tumor. *J Dent*  
16 *Res.* 2015;94(1):101-111.  
17  
18
- 19  
20 10. Kurppa KJ, Caton J, Morgan PR, et al. High frequency of BRAF V600E mutations  
21 in ameloblastoma. *J Pathol.* 2014;232(5):492-498.  
22  
23
- 24  
25 11. Sweeney RT, McClary AC, Myers BR, et al. Identification of recurrent SMO and  
26 BRAF mutations in ameloblastomas. *Nat Genet.* 2014;46(7):722-725.  
27  
28
- 29  
30 12. Brown NA, Rolland D, McHugh JB, et al. Activating FGFR2-RAS-BRAF  
31 mutations in ameloblastoma. *Clin Cancer Res.* 2014;20(21):5517-5526.  
32  
33
- 34  
35 13. Heikinheimo K, Huhtala JM, Thiel A, et al. The mutational profile of unicystic  
36 ameloblastoma. *J Dent Res.* 2018:22034518798810.  
37  
38
- 39  
40 14. Diniz MG, Gomes CC, de Sousa SF, Xavier GM, Gomez RS. Oncogenic  
41 signalling pathways in benign odontogenic cysts and tumours. *Oral Oncol.*  
42 2017;72:165-173.  
43  
44
- 45  
46 15. Gardner DG. Canine acanthomatous epulis. The only common spontaneous  
47 ameloblastoma in animals. *Oral Surg Oral Med Oral Pathol Oral Radiol Endod.*  
48 1995;79(5):612-615.  
49  
50  
51  
52  
53  
54  
55  
56  
57  
58  
59  
60

- 1  
2  
3 16. Martin M. Cutadapt removes adapter sequences from high-throughput  
4 sequencing reads. *EMBnet J.* 2011;17(1):10-12.  
5  
6
- 7 17. Kim D, Pertea G, Trapnell C, Pimentel H, Kelley R, Salzberg SL. TopHat2:  
8 accurate alignment of transcriptomes in the presence of insertions, deletions and  
9 gene fusions. *Genome Biol.* 2013;14(4):R36.  
10  
11
- 12 18. Hayward JJ, Castelhana MG, Oliveira KC, et al. Complex disease and phenotype  
13 mapping in the domestic dog. *Nat Commun.* 2016;7:10460.  
14  
15
- 16 19. Mestrinho LA. Current status and future perspectives in canine oral squamous  
17 cell carcinoma. *Vet Pathol.* 2018;55(2):200-201.  
18  
19
- 20 20. Thaiwong T, Sledge DG, Collins-Webb A, Kiupel M. Immunohistochemical  
21 characterization of canine oral papillary squamous cell carcinoma. *Vet Pathol.*  
22 2018;55(2):224-232.  
23  
24
- 25 21. Mochizuki H, Breen M. Sequence analysis of RAS and RAF mutation hot spots in  
26 canine carcinoma. *Vet Comp Oncol.* 2017;15(4):1598-1605.  
27  
28
- 29 22. Pylayeva-Gupta Y, Grabocka E, Bar-Sagi D. RAS oncogenes: weaving a  
30 tumorigenic web. *Nat Rev Cancer.* 2011;11(11):761-774.  
31  
32
- 33 23. Khanna C, Lindblad-Toh K, Vail D, et al. The dog as a cancer model. *Nat*  
34 *Biotechnol.* 2006;24(9):1065-1066.  
35  
36
- 37 24. Gibson CW, Lally E, Herold RC, Decker S, Brinster RL, Sandgren EP.  
38 Odontogenic tumors in mice carrying albumin-myc and albumin-rats transgenes.  
39 *Calcif Tissue Int.* 1992;51(2):162-167.  
40  
41  
42  
43  
44  
45  
46  
47  
48  
49  
50  
51  
52  
53  
54  
55  
56  
57  
58  
59  
60

- 1  
2  
3 25. Gomes CC, de Sousa SF, de Menezes GH, et al. Recurrent KRAS G12V  
4 pathogenic mutation in adenomatoid odontogenic tumours. *Oral Oncol.*  
5  
6 2016;56:e3-5.  
7  
8  
9
- 10 26. Mochizuki H, Kennedy K, Shapiro SG, Breen M. BRAF mutations in canine  
11  
12 cancers. *PLoS One.* 2015;10(6):e0129534.  
13  
14
- 15 27. Davanian H, Balasiddaiah A, Heymann R, et al. Ameloblastoma RNA profiling  
16  
17 uncovers a distinct non-coding RNA signature. *Oncotarget.* 2017;8(3):4530-4542.  
18  
19  
20  
21  
22  
23  
24  
25  
26  
27  
28  
29  
30  
31  
32  
33  
34  
35  
36  
37  
38  
39  
40  
41  
42  
43  
44  
45  
46  
47  
48  
49  
50  
51  
52  
53  
54  
55  
56  
57  
58  
59  
60

**Table 1.** Clinical information and *HRAS* mutation status of dogs included in this study.

Case No.	Dog breed	Sex	Age (years)	Diagnosis	Tumor/tissue location	HRAS status in tumor tissues	HRAS status in genomic DNA
1	Great Dane	Male	7	CAA	Rostral maxilla	Q61R	Wild-type
2	Samoyed	Male	12	CAA	Rostral maxilla	Q61R	Wild-type
3	Shiba Inu	Male	11	CAA	Rostral maxilla	Q61R	Not tested
4	Golden retriever	Male	10	CAA	Rostral maxilla	Q61R	Wild-type
5	Neapolitan mastiff	Male	10	CAA	Rostral mandible	Q61R	Wild-type
6	Mixed	Male	Unknown (adult)	CAA	Rostral mandible	Q61R	Not tested
7	Mixed	Male	6	CAA	Rostral mandible	Q61R	Not tested
8	Mixed	Male	12	CAA	Rostral mandible	Q61R	Not tested
9	Labrador retriever	Female	12	CAA	Rostral mandible	Q61R	Wild-type
10	Labrador retriever	Male	9	CAA	Rostral mandible	Q61R	Not tested
11	Airedale terrier	Female	10	CAA	Caudal mandible	Q61R	Wild-type
12	Labrador retriever	Male	9	CAA	Caudal mandible	Q61R	Not tested
13	Labrador retriever	Female	11	CAA	Caudal mandible	Q61R	Not tested
14	Labrador retriever	Female	8	CAA	Caudal mandible	Q61R	Wild-type
15	Staffordshire bull terrier	Female	9	CAA	Caudal mandible	Q61R	Not tested
16	Labrador retriever	Male	5	CAA	Caudal mandible	Wild-type	Not tested
17	German shorthair pointer	Female	12	OSCC	Caudal mandible	Wild-type	Not tested
18	Great Dane	Male	5	OSCC	Rostral mandible	Wild-type	Not tested
19	Boxer	Male	9	OSCC	Caudal maxilla	Wild-type	Not tested
20	Mixed	Male	12	OSCC	Rostral mandible	Wild-type	Not tested
21	Mixed	Male	4	OSCC	Rostral mandible	Wild-type	Not tested
22	Boxer	Male	12	OSCC	Rostral mandible	Wild-type	Not tested
23	Mixed	Female	10	OSCC	Caudal maxilla	Wild-type	Not tested
24	Mixed	Female	10	OSCC	Rostral maxilla	Wild-type	Not tested
25	Beagle	Male	3	Healthy gingiva	Rostral mandible	Wild-type	Not tested
26	Staffordshire bull terrier	Male	10	Healthy gingiva	Caudal mandible	Wild-type	Not tested
27	Pit-bull mix	Male	0.3	Healthy gingiva	Rostral maxilla	Wild-type	Not tested
28	Mixed	Female	Unknown (adult)	Healthy gingiva	Caudal maxilla	Wild-type	Not tested

## Figure legends

**Figure 1.** Clinical and radiographic features of CAA (A-B, dog No. 14; C-D, dog No. 16).

(A) Soft tissue mass arising from periodontal tissues on the buccal aspect of the right mandibular first molar tooth. (B) A sagittal computed tomographic image of the same animal shows that the tumor infiltrates the entire alveolus of the mesial root of the same tooth (white arrows). (C) Solid mass under seemingly intact mucosa on the buccal aspect of the right mandibular third and fourth premolar teeth. (D) An intraoral radiograph of the same dog shows the tumor deeply invading the mandible resulting in a multilocular radiographic appearance (white arrows).

**Figure 2.** Histomorphologic features of CAA. (A) Gingival mucosal biopsy with an unencapsulated, locally infiltrative, densely cellular, multicystic exophytic neoplasm composed of broad, irregular, and anastomosing islands and trabeculae of odontogenic epithelial cells interspersed with fibrovascular stroma containing small foci of mineralized woven bone tissue (arrows). (B) Higher magnification showing polygonal neoplastic cells with distinct borders, moderate amount of eosinophilic cytoplasm and small round to oval nuclei with dispersed chromatin and 1-2 inconspicuous nucleoli. Note characteristic perpendicular palisading of neoplastic columnar epithelial cells with anti-basal nuclei (reverse polarization, thick arrow) at the periphery of an island and intercellular bridges of more central cells (thin arrow). Dog No. 11, H&E.



1  
2  
3 **Figure 3.** *HRAS* p.Q61R genotyping assays on CAA tumors and paired blood. (A)  
4  
5 Sanger sequencing chromatograms of the antisense strand indicate the presence of a C  
6  
7 nucleotide (top) causing the missense Q61R mutation (dog No. 5); this mutation is not  
8  
9 evident in genomic DNA isolated from blood from the same dog (bottom). (B-D)  
10  
11 Restriction fragment length polymorphism analyses rapidly characterize sample  
12  
13 genotypes; case numbers are shown at the top of each lane. (B) HpaII cuts only the  
14  
15 mutant allele (CC**G**G); (C) BstNI cuts the wild-type allele (CC**W**GG); (D) HpaII digest on  
16  
17 genomic DNA from 7 paired blood samples confirmed that the *HRAS* p.Q61R mutation  
18  
19 is somatic and not inherited (Size ladders: pBR322 MspI in panels 3B, 3C (center), 3D;  
20  
21 10bp ladder in panel 3C (left/right)).  
22  
23  
24  
25  
26  
27

28 **Figure 4.** The percentage of oncogenic mutations in CAA (N = 16) and AM (N = 113).  
29  
30 (A) *HRAS* p.Q61R mutations in CAA as reported in the present study (maxilla N = 3;  
31  
32 mandible N = 12). One mandibular CAA case was wild-type (WT). (B) *BRAF* V600E,  
33  
34 *HRAS*, *NRAS* or *KRAS*, *FGFR2*, *SMO* and wild-type in AM (maxilla N = 27, mandible N  
35  
36 = 86) based on previous studies.<sup>10-13</sup>  
37  
38  
39  
40  
41  
42  
43  
44  
45  
46  
47  
48  
49  
50  
51  
52  
53  
54  
55  
56  
57  
58  
59  
60

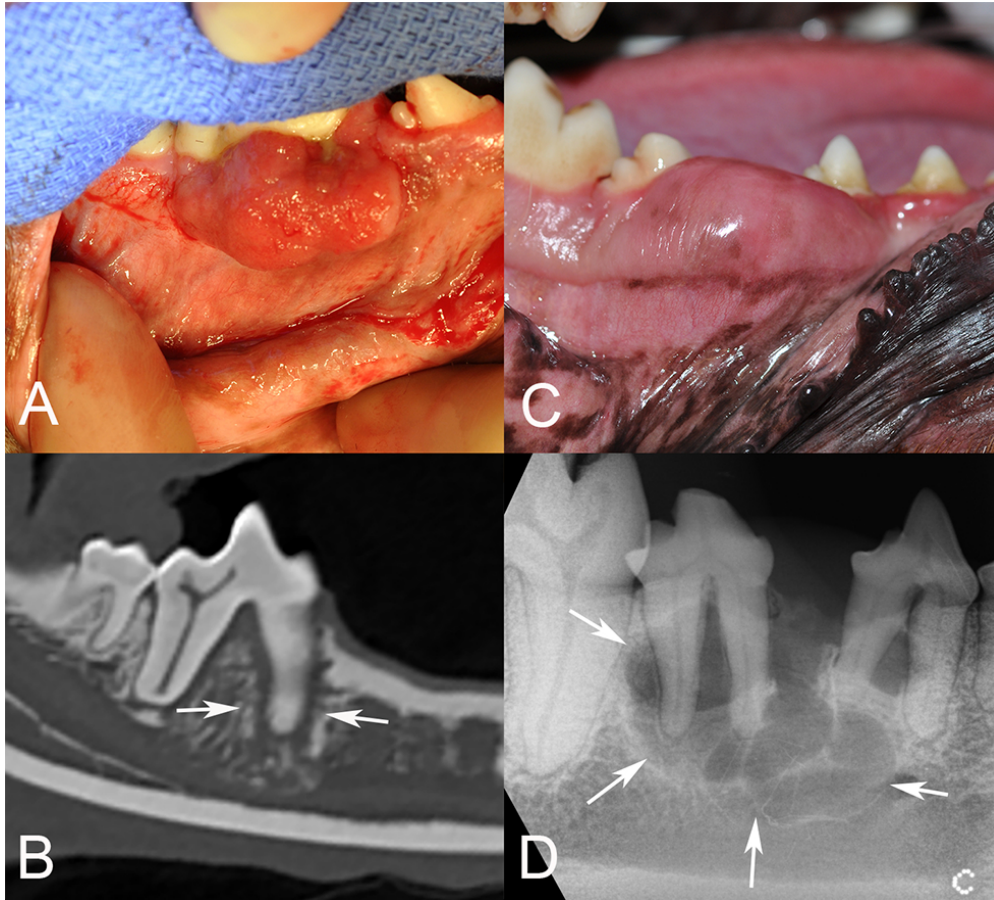


Figure 1. Clinical and radiographic features of CAA (A-B, dog No. 14; C-D, dog No. 16). (A) Soft tissue mass arising from periodontal tissues on the buccal aspect of the right mandibular first molar tooth. (B) A sagittal computed tomographic image of the same animal shows that the tumor infiltrates the entire alveolus of the mesial root of the same tooth (white arrows). (C) Solid mass under seemingly intact mucosa on the buccal aspect of the right mandibular third and fourth premolar teeth. (D) An intraoral radiograph of the same dog shows the tumor deeply invading the mandible resulting in a multilocular radiographic appearance (white arrows).

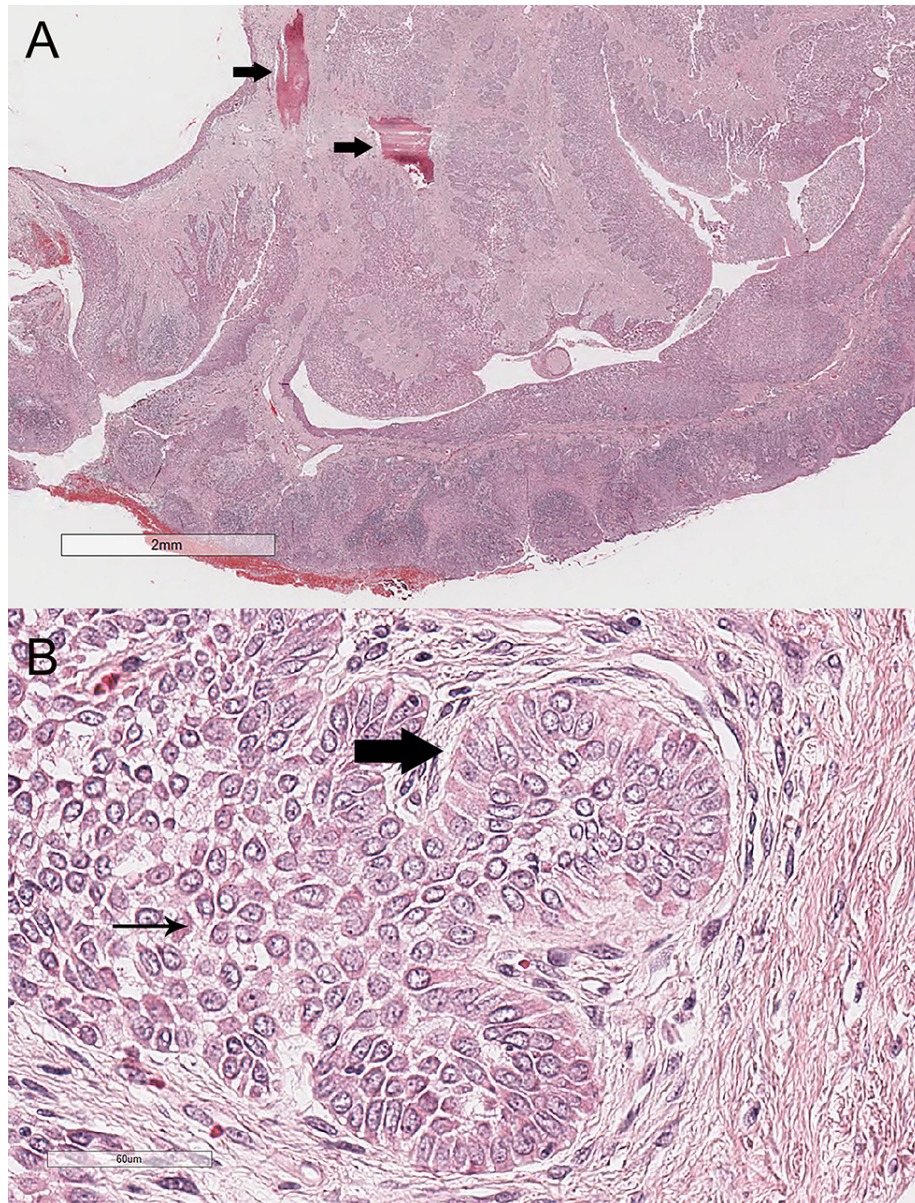


Figure 2. Histomorphologic features of CAA. (A) Gingival mucosal biopsy with an unencapsulated, locally infiltrative, densely cellular, multicystic exophytic neoplasm composed of broad, irregular, and anastomosing islands and trabeculae of odontogenic epithelial cells interspersed with fibrovascular stroma containing small foci of mineralized woven bone tissue (arrows). (B) Higher magnification showing polygonal neoplastic cells with distinct borders, moderate amount of eosinophilic cytoplasm and small round to oval nuclei with dispersed chromatin and 1-2 inconspicuous nucleoli. Note characteristic perpendicular palisading of neoplastic columnar epithelial cells with anti-basal nuclei (reverse polarization, thick arrow) at the periphery of an island and intercellular bridges of more central cells (thin arrow). Dog No. 11, H&E.

This is the peer reviewed version of the following article: Peralta, S, McCleary-Wheeler, AL, Duhamel, GE, Heikinheimo, K, Grenier, JK. Ultra-frequent HRAS p.Q61R somatic mutation in canine acanthomatous ameloblastoma reveals pathogenic similarities with human ameloblastoma. *Vet Comp Oncol.* 2019; 17: 439– 445, which has been published in final form at <https://doi.org/10.1111/vco.12487>. This article may be used for non-commercial purposes in accordance with Wiley Terms and Conditions for Use of Self-Archived Versions.

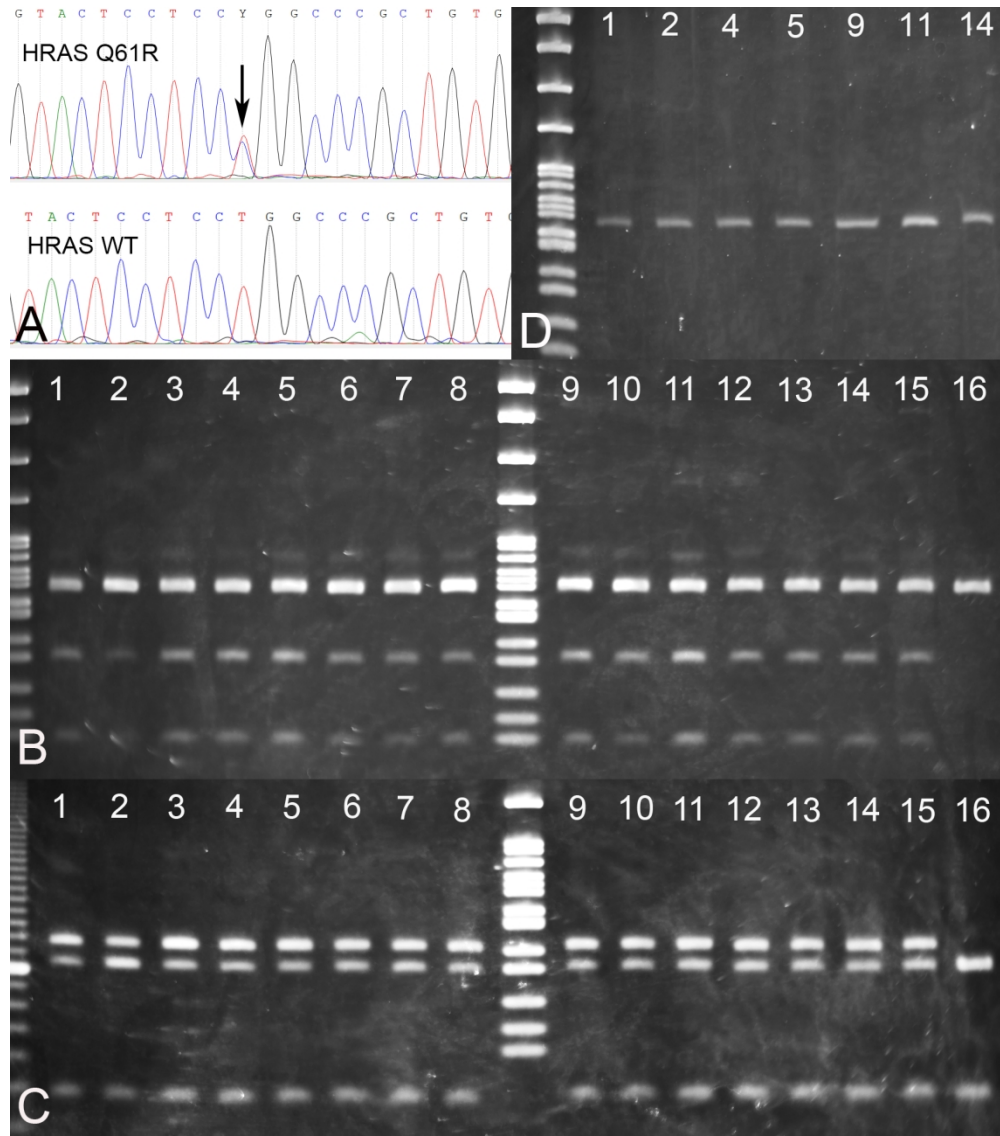


Figure 3. HRAS p.Q61R genotyping assays on CAA tumors and paired blood. (A) Sanger sequencing chromatograms of the antisense strand indicate the presence of a C nucleotide (top) causing the missense Q61R mutation (dog No. 5); this mutation is not evident in genomic DNA isolated from blood from the same dog (bottom). (B-D) Restriction fragment length polymorphism analyses rapidly characterize sample genotypes; case numbers are shown at the top of each lane. (B) HpaII cuts only the mutant allele (CCGG); (C) BstNI cuts the wild-type allele (CCWGG); (D) HpaII digest on genomic DNA from 7 paired blood samples confirmed that the HRAS p.Q61R mutation is somatic and not inherited (Size ladders: pBR322 MspI in panels 3B, 3C (center), 3D; 10bp ladder in panel 3C (left/right)).

This is the peer reviewed version of the following article: Peralta, S, McCleary-Wheeler, AL, Duhamel, GE, Heikinheimo, K, Grenier, JK. Ultra-frequent HRAS p.Q61R somatic mutation in canine acanthomatous ameloblastoma reveals pathogenic similarities with human ameloblastoma. Vet Comp Oncol. 2019; 17: 439– 445, which has been published in final form at https://doi.org/10.1111/vco.12487. This article may be used for non-commercial purposes in accordance with Wiley Terms and Conditions for Use of Self-Archived Versions.

1  
2  
3  
4  
5  
6  
7  
8  
9  
10  
11  
12  
13  
14  
15  
16  
17  
18  
19  
20  
21  
22  
23  
24  
25  
26  
27  
28  
29  
30  
31  
32  
33  
34  
35  
36  
37  
38  
39  
40  
41  
42  
43  
44  
45  
46  
47  
48  
49  
50  
51  
52  
53  
54  
55  
56  
57  
58  
59  
60



Figure 4. The percentage of oncogenic mutations in CAA (N = 16) and AM (N = 113). (A) HRAS p.Q61R mutations in CAA as reported in the present study (maxilla N = 3; mandible N = 12). One mandibular CAA case was wild-type (WT). (B) BRAF V600E, HRAS, NRAS or KRAS, FGFR2, SMO and wild-type in AM (maxilla N = 27, mandible N = 86) based on previous studies.10-13

791x395mm (72 x 72 DPI)